

# Some Results of Aerosol and Radiation Measurements in Siberia Under the SATOR Program of the IAO

V. V. Zuev, B. D. Belan, Yu. A. Pkhalagov, and S. M. Sakerin  
Institute of Atmospheric Optics, Tomsk, Russia

## Introduction

The SATOR Program of the Institute of Atmospheric Optics (IAO) started in 1991. Due to interaction with the ARM Program, the specific weight of radiation measurements in the SATOR Program has been increased significantly for two years.

The investigation of gases, aerosols, and radiation regime of the atmosphere with regard for their interrelations for typical regions of the earth is one of the most important radiation-climatic problems. Among the typical regions, the zone of boreal forests of moderate latitudes should be separated, which covers the considerable territory of the Eurasian and American continents (including the West Siberia). The following geophysical factors are characteristic of these regions:

- high density of forests and plant canopy with a corresponding albedo and specifics of aerosol-gas transformations and interactions
- relatively low anthropogenic load
- closeness to the arctic zone, whose atmosphere features low content of aerosol and moisture.

In this report we consider some results of simultaneous measurements of aerosol concentration and meteorological parameters in the near-ground atmosphere in different seasons in order to find the main factors governing formation and transformation of the atmospheric aerosol. To this end, we also analyze the optical measurement data on the spectral coefficients of visible and IR radiation extinction due to aerosol in atmospheric hazes.

To study the character of variability of radiation fluxes, the data of investigations of aerosol and water vapor total contents in the atmosphere are considered.

Tabulated in Table 1 are the coefficients of correlation between the variations in different-size aerosol particle

**Table 1.** The coefficients of correlation between the meteorological parameters and aerosol in 1994.

	Winter (n > 28000)	
Nd, $\mu\text{m}$	Water vapor pressure	Temperature
0.4	-0.110	-0.110
0.6	-0.209	-0.179
0.8	-0.195	-0.153
1.0	-0.151	-0.108
1.5	-0.172	-0.102
2.0	-0.113	-0.057
$\Sigma\text{N}$	-0.146	-0.155
	Summer (n > 35000)	
Nd, $\mu\text{m}$	Water vapor pressure	Temperature
0.4	-0.051	0.049
0.6	-0.058	0.129
0.8	0.001	0.175
1.0	0.112	0.116
1.5	0.149	0.192
2.0	0.166	0.202
$\Sigma\text{N}$	-0.034	0.093

number density and variability of the meteorological parameters in the near-ground atmospheric layer for winter (28000 events) and summer (35000 events) conditions. The significant correlation coefficient is 0.1038 with probability 0.9995 or 0.052 with probability 0.9500.

In winter a stable negative correlation is observed between all aerosol fractions and the water vapor pressure and the temperature. This fact reflects the domination of the condensation processes in the aerosol generation in this season. The relative humidity has a significant positive relation with the most fine-disperse aerosol fraction and a

negative one with the medium-disperse fraction ( $d = 1.5\text{--}2.0 \mu\text{m}$ ). The former is indicative of the same mechanisms of generation of water vapor and aerosol in the near-ground layer, while the latter accounts for the sink of water vapor on particles.

In the summer period (Table 1b) the view of the correlation coefficient between water vapor pressure and aerosol is somewhat different. A slight negative correlation with the submicron fraction remains in it and in addition a stable positive correlation with the medium-disperse fraction appears. Conceivably a portion of water vapor might go to form particles. The air temperature in summer has a stable positive relation with aerosol; this relation becomes stronger with increasing size of particles. It reflects the well-known fact that under positive temperatures a greater amount of aerosol-forming vapors comes and coagulation and photochemical processes intensify.

The data listed in Table 1 agree well with the results of long-term measurements of the spectral transmittance of the atmosphere along the near-ground path about 1000 m long in the  $0.44\text{--}11.5 \mu\text{m}$  wavelength range.

Shown in Figure 1a are the averaged spectral dependences of the coefficients of aerosol extinction in a winter haze (curve 1) and an ice fog (2) which is usually observed under anticyclone conditions at the air temperature  $t \leq -15^\circ\text{C}$ . It should be noted that an ice fog only increases the level of aerosol extinction throughout the entire wavelength range and practically does not change its spectral structure. Such

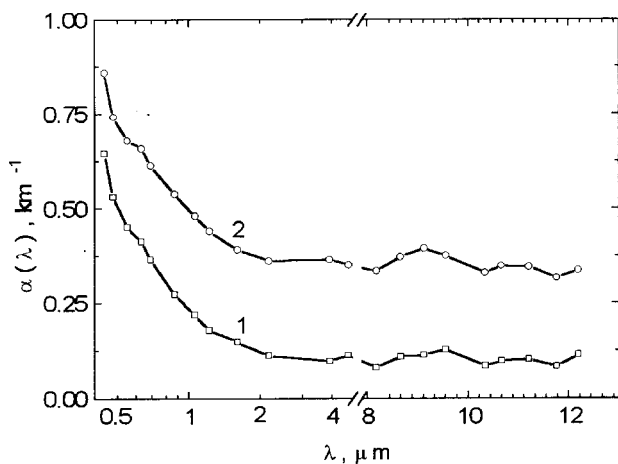


**Figure 1a.** Averaged spectral dependence of the aerosol extinction coefficients under winter conditions: winter haze (1) and ice fog (2) at the temperature  $t \leq 15^\circ\text{C}$ .

a behavior is in agreement with the stable negative correlation between all aerosol fractions and the water vapor pressure and the temperature (Table 1a).

Shown in Figure 1b are the averaged spectral dependences of the coefficients  $\alpha(\lambda)$  in summer hazes obtained in the former part of June (curve 1,  $t = 12.2^\circ\text{C}$ ) and in July (curve 2,  $t = 23.8^\circ\text{C}$ ). It is clearly seen from the figure that curves 1 and 2 differ dramatically both in the level of coefficients  $\alpha(\lambda)$  and in their spectral runs. Such a behavior of the curves also agrees well with that of the coefficients of correlation between the medium-disperse aerosol fraction ( $d \geq 1.0 \mu\text{m}$ ) and the water vapor pressure and the temperature (Table 1b). On the whole, the run of the all four curves corresponds to the annual run of aerosol concentration in the near-ground atmospheric layer with the maximum in the winter period (Figure 2).

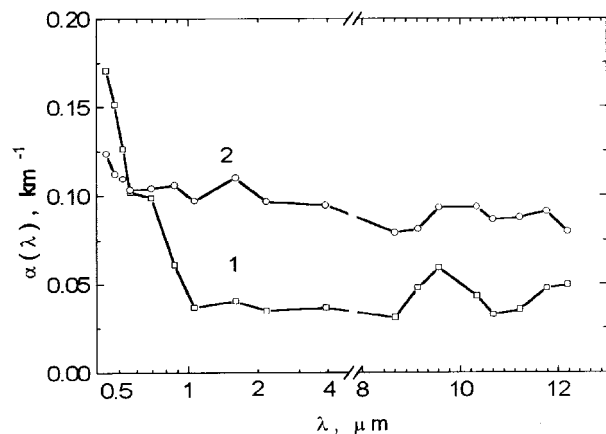


**Figure 1b.** Averaged spectral dependence of the aerosol extinction coefficients in summer hazes: 1) June ( $t = 12.2^\circ\text{C}$ ), 2) July ( $t = 23.8^\circ\text{C}$ ).

Beginning in 1992, within the framework of the SATOR Program the investigations were started into the regularities of variability of the aerosol optical depth (AOD) and columnar water vapor (CWV) in the atmosphere at the scales from mesometeorological to global. Simultaneously with measuring the atmospheric parameters, the observations were conducted over the characteristics of incoming radiation: global, diffuse, and direct (including the spectral one) solar radiation as well as the sunshine duration (SD).

The statistical analysis of the results obtained during the period of researches (1992–1995) has shown that AOD varies within one order of magnitude from 0.04 to 0.5 with the mean value about 0.2 ( $\lambda \approx 0.5 \mu\text{m}$ ). The relative variability of the aerosol turbidity was 30–50% for the entire wavelength range

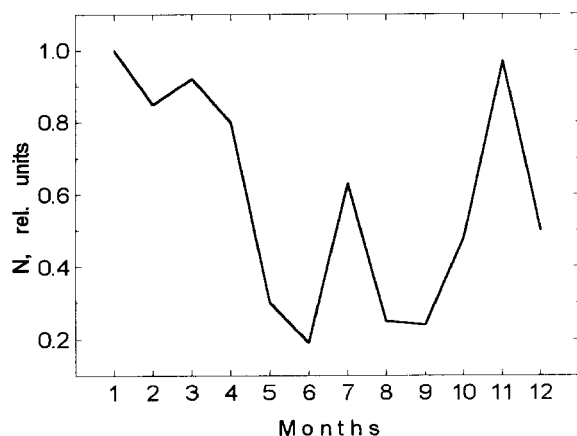


**Figure 2.** The normalized annual variations of aerosol mass concentration in Tomsk.

(0.37–1.06  $\mu\text{m}$ ) and all seasons. The histograms of the repetition have an unimodal character with a positive asymmetry. When analyzing the AOD variability, the interannual trend has been revealed caused by the postvolcanic (Pinatubo 1991) relaxation of the atmosphere to the background state. The quantity of the trend, for example, for June values of AOD averaged over the three-year period was 70%. Seasonal variability of the atmospheric transmittance during the period of researches was distorted (and smoothed) by the evolution of the volcanic layer.

The greatest contribution to variations of the aerosol turbidity was made by the variations of synoptic and global scales (with the amplitude of 0.3 and greater). In the frequency spectrum of AOD (Figure 3) one can see a series of maxima (3, 4, 5, 7, 8, 12, 20 days) that correspond a lifetime of synoptic objects and cycles of zonal circulation of the moderate latitudes. In the diurnal run of AOD (Figure 4) for the summer period, the following sections can be separated: (a) the morning section (up to 12.00) with the small AOD value and its slight variability, (b) the day increase of turbidity with the rate  $\approx 3\%$  per hour, and (c) the slightly pronounced drop of AOD after 18.00. The general amplitude of the relative diurnal variability is about 20%.

The main contribution to the CWV variability is made by the seasonal variations: in monthly averaged values the region of CWV variations is from 0.48  $\text{g}/\text{cm}^2$  in December to 2.76  $\text{g}/\text{cm}^2$  in July. The maximum amplitude of the short-period oscillations nearly reaches that of seasonal variations of the CWV. Compared to the AOD, the relative variability of the CWV is within more narrow range of 35 to 45%. In the frequency spectrum, the maxima of synoptic oscillations (periods of 4, 5, and 7–8 days) are similar to those for AOD,

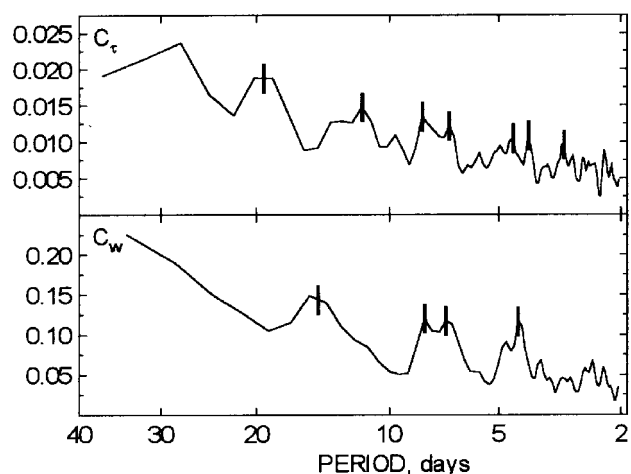


**Figure 3.** Periodograms of the short-period oscillations of the AOD (a) and the CWV (b); vertical bars show the characteristic maxima.

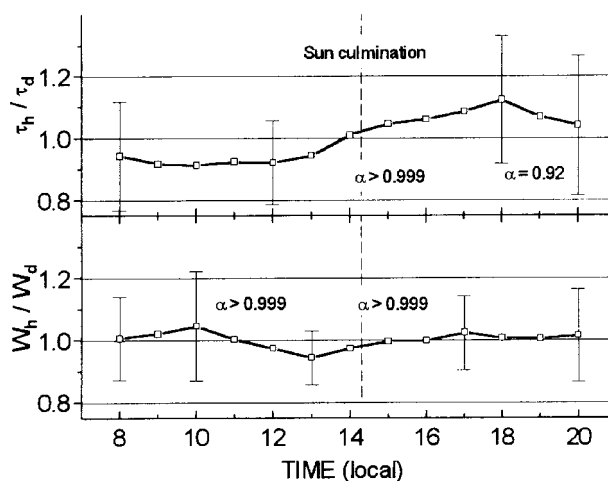


**Figure 4.** The relative diurnal run of the AOD (a) and the CWV (b) shown as average-annual values  $\tau_h$  normalized to average-diurnal values  $\tau_d$ ;  $\alpha$  is the confidence probability of the significance of  $\tau_h/\tau_d$  differences according to the Student criterion.

whereas for global oscillations only one intermediate value ( $\approx 15$  days) can be separated. The diurnal run of water content is less pronounced as compared to that of aerosol. The general amplitude is about 10% with the maximum at 10.00 and the minimum at 13.00. The diurnal variability of the CWV qualitatively follows the run of the near-ground humidity. In contrast to the latter, the midday maximum is connected with the outflow of water vapor into cloudiness. In general, the CWV well correlates with the humidity in the

near-ground layer. The correlation with the water vapor pressure is nearly linear with the coefficient of mutual correlation of 0.878.

Aerosol, columnar water vapor, and cloudiness have a complex and different effect upon different components of the incoming radiation. As an example, Table 2 presents the coefficients of mutual correlation of the AOD ( $\tau_{0.48}^a$ ), the CWC ( $w$ ) and the sunshine duration ( $S_s$ ) with the diurnal sums of the global radiation ( $Q_\Sigma$ ), the diffuse radiation ( $D_\Sigma$ ), and the direct radiation ( $S^2$ ) reduced to the atmospheric mass-2 (according to the data of 1994).

**Table 2.** The coefficients of mutual correlation of AOD at  $0.48 \mu\text{m}$  ( $\tau_{0.48}^a$ ), CWV ( $w$ ), SD ( $S_s$ ) with the diurnal sums of the global solar radiation ( $Q_\Sigma$ ), diffuse radiation ( $D_\Sigma$ ), and the direct radiation ( $S^2$ ) reduced to the atmospheric mass-2.

	$(\tau_{0.48}^a)$	$w$	$S_s$	$Q_\Sigma$	$D_\Sigma$	$S^2$
$(\tau_{0.48}^a)$	1	0.40	0.22	0.16	0.16	-0.77
$w$		1	-0.31	-0.40	0.29	-0.71
$S_s$			1	0.94	-0.53	-0.19
$Q_\Sigma$				1	-0.51	-0.007
$D_\Sigma$					1	-0.25
$S^2$						1

The maximum correlation between  $Q_\Sigma$  and the sunshine duration (SD) confirms the principal effect of cloudiness upon the variability of the incoming radiation, as well as the possibility to use the SD for estimating the total radiation.

The direct radiation is characterized by the high level of correlation with the two other atmospheric parameters: AOD and CWV. The diffuse radiation correlates only slightly with the SD (the small values of SD correspond to a large cloud fraction and an increase in the scattered radiation). At the

level of significance (0.4 with the confidence probability of 0.95) is the correlation between  $Q_\Sigma$  and the water content as well as that between the atmospheric parameters  $\tau^a$  and  $w$ .

Diurnal behavior of  $S_\lambda$  value shown in Figure 5 (spring, 1993) reveals, along with the regular astronomic factor (increase of solar radiation flux by noon), certain peculiarities in the diurnal behavior of the atmospheric transmission. Thus, in the diurnal behavior of  $S_\lambda$  in May we can observe asymmetry and decreased radiation values, except for morning hours. Such a behavior of  $S_\lambda$  is connected, with the snow melting in the morning as well as with the increase of convection and atmospheric turbidity because of aerosol and water vapor.

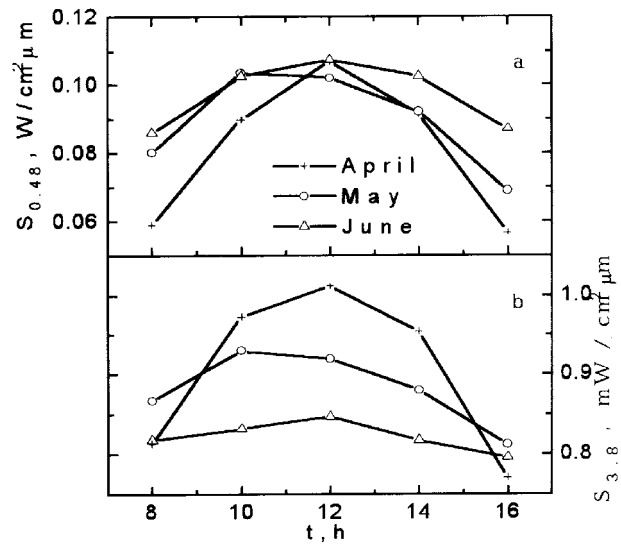


**Figure 5.** The mean behavior of radiation  $S_{0.48}$  (a) and  $S_{3.8}$  (b).

From the results obtained it follows that for April and May the variance of the radiation variation,  $S_\lambda$ , increases from morning to evening and in June, in the afternoon, its decrease is observed.

The effect of atmospheric factor in May turned out to be stronger than the expected increase of direct radiation due to higher sun (the  $S_\lambda$  values in May are lower than those in April).